New instruments and technologies for Cultural Heritage survey: full integration between point clouds and digital photogrammetry

F. Rinaudo[a], F. Chiabrando[b], F. Nex[a], D. Piatti[a]

[a]DITAG/POLITECNICO DI TORINO, Corso Duca degli Abruzzi, 24, 10129 Torino, Italy (fulvio.rinaudo, francesco.nex, dario.piatti)@polito.it
[b]DINSE/POLITECNICO DI TORINO - Viale Mattioli 39, 10125 Torino, Italy - filiberto.chiabrando@polito.it

Abstract. In the last years the Geomatic Research Group of the Politecnico di Torino faced some new research topics about new instruments for point cloud generation (e.g. Time of Flight cameras) and strong integration between multi-image matching techniques and 3D Point Cloud information in order to solve the ambiguities of the already known matching algorithms. ToF cameras can be a good low cost alternative to LiDAR instruments for the generation of precise and accurate point clouds: up to now the application range is still limited but in a near future they will be able to satisfy the most part of the Cultural Heritage metric survey requirements. On the other hand multi-image matching techniques with a correct and deep integration of the point cloud information can give the correct solution for an "intelligent" survey of the geometric object break-lines, which are the correct starting point for a complete survey. These two research topics are strictly connected to a modern Cultural Heritage 3D survey approach. In this paper after a short analysis of the achieved results, an alternative possible scenario for the development of the metric survey approach inside the wider topic of Cultural Heritage Documentation is reported.

Keywords: ToF camera, calibration, matching, multi-image, digital photogrammetry, LiDAR

1 Introduction

The close range metric survey approach has been completely renovated thanks to the developments of LiDAR and multi-image matching (digital photogrammetry) techniques. While in the past a metric survey was an intelligent, rational, and manual selection of the points needed to describe the shape of the surveyed object, today the above mentioned techniques force the surveyors to work with point clouds acquired without any understanding of the object shape. Starting from this "not-intelligent" geometry the user has to interpret and describe the searched shapes.

The rapid development of the research studies in the fields of point cloud management and interpretation, by using segmentation and modeling algorithms and/or by using some of the information extracted from oriented images, has allowed

the production of traditional (technical drawings such as plans and sections) and innovative (true orthophoto, solid images, 3D realistic models) representation instruments. In the last few years, the research group of Geomatics of the Politecnico di Torino has developed specific research projects considering two different aspects: testing and calibration of new instruments able to generate 3D point clouds and a full integration between point clouds and multi-image matching techniques.

The first topic aims to reduce the time needed to acquire dense point clouds and the costs of the needed instrumentation on the survey budget; the second topic aims to re-evaluate digital photogrammetry as the more suitable technique to produce dense and affordable information if helped by a rough shape model of the surveyed object especially in Cultural Heritage applications.

2 ToF cameras

Time of Flight (ToF) cameras (also known as 3D cameras or Range cameras) represent a rather new way to obtain 3D point clouds, which are almost comparable with those of traditional LiDAR acquisitions. Using these cameras, a bundle of distances is determined simultaneously (at video frame rates) for each pixel of a two-dimensional sensor array. Although ToF cameras are usually characterized by no more than a few thousands of tens of pixels, a maximum unambiguous measurement range up to 30 m can be reached and complete 3D point clouds of the analyzed objects can be quickly acquired (the sampling rate can reach more than 50 frames/s).

These devices allow to generate point clouds such as in the case of the LiDAR technique and photogrammetric matching but with the great advantage of real time acquisition, low cost (approximately $1/10^{th}$ of the standard price of a LiDAR equipment) and handiness. Unlike photogrammetric techniques, 3D cameras allow a point cloud to be obtained of the object which has to be surveyed from even only one point of view, without the need of any particular lighting conditions, since these cameras are active sensors that work outside of the visible spectrum.

Two main variations of the ToF principle have been implemented above all in 3D cameras: one measures distances by means of direct measurement of the runtime of a travelled light pulse using arrays of single-photon avalanche diodes (SPADs) [1] [16]; the other method uses amplitude modulated light and obtains distance information by measuring the phase difference between a reference signal and the reflected signal [8] [9]. While complex readout schemes and low frame rates have prevented the use of SPAD arrays in commercial 3D-imaging products up to now, the second category has already been implemented successfully in several commercially available 3D camera systems. More information about pixel structures and performance limitations of these sensors can be found for instance in [3].

ToF cameras usually deliver a range image and an amplitude image with infrared modulation intensities: the range image (or depth image) contains for each pixel the radial measured distance between the considered pixel and its projection on the surveyed object, while the amplitude image contains for each pixel the strength of the reflected signal. In some cases an intensity image is also delivered, which represents the mean of the total light incident on the sensor (reflected modulated signal and

background light of the observed scene).

Each 3D camera is usually equipped with a standard calibration but, as reported in different works [14][16] and in our previous tests [16] the distance measurements of ToF cameras are still affected by some residual systematic errors which can have the same extent of the precision of the instrument.

In Table 1 the main technical specifications of some commercial ToF cameras are reported.

Table 1. Technical specification of some commercial ToF cameras

Camera	Sensor [px x px]	Meas. range [m]	Accuracy [m]	Weight [kg]
CAM CUBE 2.0	204 x 204	0.3 ÷ 7	± 0.01÷0.03	1.438
SR-4000	176 x 144	0.3 ÷ 10	± 0.015	0.470
OPTRICAM DS10K-A	120 x 90	0.3 ÷ 10	± 0.03	n.a.
FOTONIC B70	160 x 120	0.1 ÷ 7	± 0.015	1.049

Table 2. SR-4000 camera specifications (http://www.mesa-imaging.ch – accessed 10th June 2010).

Pixel array size [-]	176 (h) × 144 (v)
Field of view [°]	43.6 (h) × 34.6 (v)
Pixel pitch [µm]	40
Illumination wavelength [nm]	850
Working range [m]	0.3 ÷ 5.0
Maximum frame rate [fps]	54
Dimensions [mm]	65 × 65 × 68
Weight [g]	470

In the following sections some of the tests performed by our Research Group on the SR-4000 camera are summarized.

2.1 ToF camera calibration

The more recent 3D cameras are usually provided with a calibration model of the measured distances in order to correct most of the biases related to their electronic components. In order to check the measurement accuracy which can be obtained on a real object, the following test has been performed.

An architectural artifact (a decorated frame) has been surveyed by using a triangulation based scanner (MENSI S10) which guarantees an accuracy of about 0.1 mm at a taking distance of 2 m (see Fig. 1 left). The obtained 3D point cloud can be considered as the "truth" since the MENSI S10 accuracy is less than 1/10th of the expected accuracy of the SR-4000 camera. The same object has been surveyed by

using the SR-4000 camera (see Fig. 1 right), acquiring and averaging thirty frames in order to reduce the measurements noises of the single frame acquisition. Then, the obtained 3D point cloud has been compared with the previous one. Before the acquisition, the camera has been used for a continuous acquisition of about 40 minutes (warm up time) in order to reach a good measurement stability [16].

Fig. 1. The MENSI S10 and SR-4000 camera record the decoration

In order to compare the two point clouds, they have to be defined in a unique coordinate system: therefore, seven control points (the white cubes visible in Fig. 1) have been positioned inside the acquired scene and used to register the SR-4000 point cloud in the same coordinate system of the MENSI S10 point cloud. The estimated discrepancies can be interpreted as a residual variable that, by theory, has a null mean and a mean square error equal to the measurement precision if the measurements are accurate and precise. In Fig. 3 (RIGHT top) a representation of the estimated discrepancies on the architectural decoration is reported with an arbitrary color scale. In this case, a mean value and a standard deviation value of the differences of 0.006 m and 0.011 m have been obtained respectively. Therefore, a residual systematic effect is still present inside the camera measurements. Its amount is not acceptable since it is very close to the declared measurement precision of 5 mm: the calibrated 3D camera is precise but not accurate enough. In order to overcome this problem, an extra self-calibration model has been developed, which increases the SR-4000 measurement accuracy.

The model is described by the following equation:

$$e = \lambda_0 + \lambda_1 \cdot d \cdot \sin(\lambda_2 \cdot d + \lambda_3) \tag{1}$$

where: d is the pixel measured distance, λ_0 is a constant error, λ_1 represents a scale factor which multiplies a "wiggling error" modeled by a sinusoidal function (λ_2 = angular frequency, λ_3 = phase shift).

The values of the calibration model parameters have to be estimated by using a reference plain placed at know distances [16]. These parameters can be considered stable for the camera, however the calibration should be repeated every year in order to check the stability of the instrument. Coming back to the previously described test, the 3D point cloud acquired with the SR-4000 camera has been corrected by using the proposed calibration model and a new estimation of the discrepancies against the 3D point cloud of the MENSI S10 has been performed.

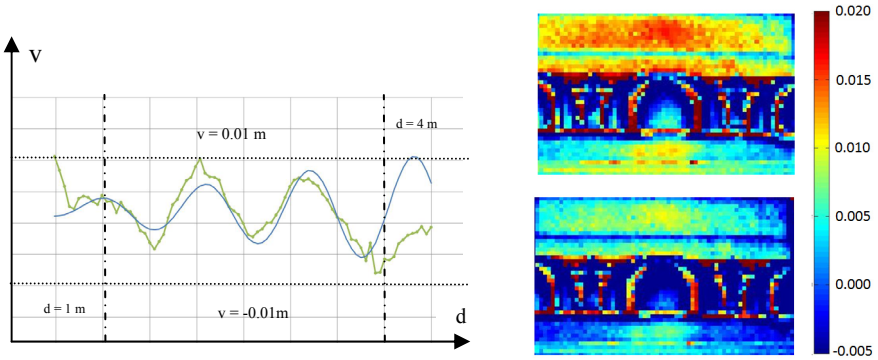

Fig. 2. LEFT: Experimental discrepancies *v* (green line) and proposed calibration model (blue line) – RIGHT: Discrepancies between the MENSI S10 point cloud and the SR-4000 point cloud before (top) and after (bottom) applying the extra calibration model (scale bar in meters).

In this case the mean value of the discrepancies falls down to 0.001 m, while the standard deviation is the same of the previous one. In Fig. 2 (RIGHT bottom) a representation of the estimated discrepancies on the architectural decoration after applying the calibration model is reported with an arbitrary color scale.

Considering the theory of the residual variable, it is possible to state that, after the proposed self-calibration, the SR-4000 camera is able to produce more accurate measurements with a precision that is close to the declared technical specification (see Tab. 2).

2.2 A complete survey

The SR-4000 camera has been used in a standard survey procedure to generate a realistic 3D model of a window, applying the self-calibration model on the four acquired point clouds.

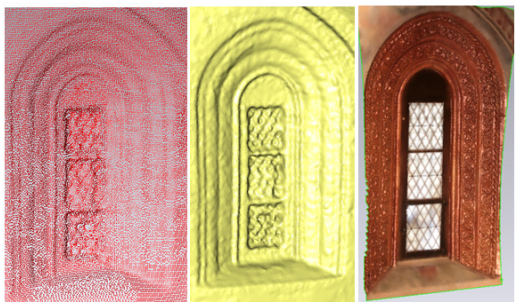

Fig. 3. Point cloud (left), mesh model (centre), textured final model (right)

A digital image has been acquired by means of a calibrated CANON EOS 5D MARKII camera: this image has been oriented in the same coordinate system of the

ToF point cloud by using some reference points.

The processing of the point cloud necessary to reach the mesh model of the window has been performed by using the *Geomagic Studio*® software; the model has been finally coloured by using the radiometric information extracted from the digital image. Fig. 3 shows the obtained results.

2.3 First conclusions

3D cameras represent an affordable solution to be used instead of the traditional LiDAR approach to produce point clouds useful to provide the primary data for modeling small and medium sized objects.

The proposed self-calibration model refines the distance measurement accuracy between 0.5 m and 4.0 m of the camera to object distance, therefore only small objects can be surveyed with a static acquisition.

The high sampling rate of the SR-4000 camera allows to conceive a possible use as a 3D video-camera in order to record data on larger objects (e.g. a room, a statue, etc.): in this case a real-time ICP based registration of the video frames could be developed in order to allow an easy and self controlling acquisition.

In any case, the ToF point clouds have to be corrected by using a self-calibration model whose parameters can be estimated with a suitable calibration procedure like the one adopted by the authors [16].

3 Lidar/digital photogrammetry integration

When we talk about LiDAR and digital photogrammetry integration we actually mean the possibility to overcome the limits of LiDAR technology by using some information coming from digital photogrammetry (e.g. realistic 3D model, manual understanding of break-lines, etc.) or to extend the photogrammetric procedure thanks to the information coming from LiDAR data (e.g. true orthophoto generation).

These applications define the lowest level of possible integrations: it can be stated that digital photogrammetry, especially in Cultural Heritage applications, can provide useful results (by paying many manual interventions) even without LiDAR integration. On the other hand, LiDAR without any help from digital photogrammetry cannot give satisfactory solutions to the 3D metric survey.

In addition, LiDAR technology uses a not self-controlled survey strategy: the three coordinates of a generic point are estimated by using just three independent measurements, therefore, a correct estimation of the achieved accuracy is not possible. On the contrary, photogrammetry estimates 3D coordinates of a generic point by using at least four independent measurements (in the case that only two overlapping images are used). Then, in a modern approach of digital photogrammetry the multi-image matching allows the estimation of the 3D coordinates of a generic point also by using three or more overlapping images: this means that the three unknown coordinates are estimated in a least squares approach with at least six independent equations. Therefore, the redundancy that a multi-image approach allows is equal to the number of the unknowns and, from a statistical point of view, this is the

best condition for a correct estimation of the precision.

3.1 Multi-image matching

The automated extraction of objects from photogrammetric images has been a topic of research for decades. Nowadays, image-matching techniques allow a great number of points to be extracted in a quick way. In particular, multi-image techniques allowed obtaining a point cloud density comparable to the LiDAR one. Then, they allow an improvement in the geometric precision and the reliability with respect to image pairs, by extracting points and edges from images and projecting their match in the space [17]. Actually, this kind of solution requires an approximate DSM in order to "drive" the solution to the correct match; the more accurate is this model, the more correct (without blunders) is the solution.

These techniques consider the epipolar geometry between images in order to reduce the search area in adjacent images, and, thus, decreasing the number of blunders to a great extent. The run along the epipolar line is further reduced by the z-value that is provided by an approximate 3D model. The needed approximation increases with the ratio between the depth differences (Z-values) and the taking distance and with the decreasing of the base/taking distance ratio of the overlapping used images.

Therefore in Cultural Heritage applications, where large values of the Z/taking-distance are present (e.g. façades are usually rough with balconies, columns or decorations that protrude of several meters), these variations are more relevant as they can be greater than 1/5 of the taking distance. In these conditions, multi-image matching can have the right help just by using dense and accurate 3D models.

These 3D models can be produced by LiDAR instruments or, as we demonstrated in the previous sections, by means of the ToF cameras. Therefore, instead of talking about LiDAR and digital photogrammetry integration, it is possible to generalize the concept saying that digital photogrammetry needs a closed Point-Cloud integration.

3.2 Point clouds and digital photogrammetry integration

Fig.4 shows the flow-chart of a standard multi-image matching process integrated with a correct use of an approximate point cloud in order to overcome the ambiguity of the standard matching procedure. The point cloud can be produced by using LiDAR or ToF cameras, as mentioned before.

The goal of this approach is to try to satisfy the needs of the final users (photogrammetrists, surveyor, architects, engineers, archaeologists) reducing the time needed to reach the final products. In particular, façade break-lines are automatically extracted in the space in order to ease and limit the manual intervention in the post processing phases.

The images are acquired according to an *ad hoc* taking configuration (Figure 9): several images are acquired and the most central one is considered as reference image during the matching process [17]. The point cloud is acquired from a central position with respect to the image acquisition in order to have approximately the same

occluded areas in the Point Cloud data and in the reference image.

The acquired images are pre-processed according to an auto-adaptive smoothing. Then, they are enhanced using a Wallis filter; this filter is able to sharpen the radiometric boundaries and to enhance the edges.

The orientation is performed in a local coordinate system. In this step, the A^2SIFT (Auto-Adaptive Scale Invariant Feature Transform) operator [16] is adopted in the tie-point extraction and a robust (Least Median Square) relative orientation is then performed in order to eliminate the mismatches [16]. Finally, a bundle block adjustment is performed.

After that, the edge extraction is performed by the Canny operator on the reference image. The extracted edges are then approximated, by identifying the pixels where the edge changes in direction (e.g. knots) and linking these dominant points by straight edges.

The edges are only extracted in the regions of interest: façade glass is always excluded as it could create mismatches and blunders due to reflection.

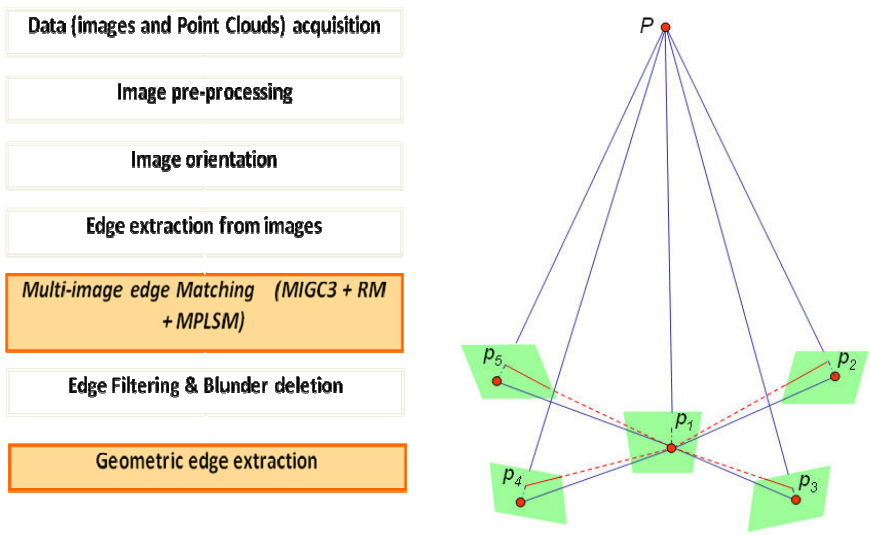

Fig. 4. Multi-Image matching process enhanced by Point Cloud integration (colored boxes) and suggested image taking strategy

The point cloud is registered in the photogrammetric coordinate system. In this way, the information between the images and the point cloud are shared.

Then, a multi-image matching algorithm is set up: this step can be divided in three different algorithms. The first algorithm ($MIGC^3$) is similar to the Geometrically Constrained Cross Correlation (GC^3) [17] and it is used to define a pixel accuracy location of the homologous points.

The images are preliminarily corrected (using the camera inner calibration) in order to ease them into a central perspective.

Then, the algorithm uses a multi-image approach by considering a reference image

and projecting the image patch of each dominant point of the reference image onto the point cloud. Using the approximate Z-value achieved by the point cloud interpolation, it back-projects the image patch onto the other images, giving an approximate position of the homologous points.

The epipolar constraint limits the search space in the images. The length of this line could be achieved considering the Z-value given by the point cloud; then, in order to find the homologous points in all the images, this value is varied into a range (Δz). This work can be further enforced and improved through the position of the already matched points: the Z-value of two adjacent dominant points being on the same edge must be similar. In this way, it is possible to reduce the length of the epipolar line on the object to few centimeters [14].

Through this algorithm, the dominants points of each edge are matched in all the images in order to reconstruct the break-line 3D position.

Even if MIGC^3 is able to match a high percentage of the extracted dominant points, some dominant points can have more than one possible match in terms of cross correlation. In order to solve these ambiguous matching and to improve the rate of the successfully matched points, the relational matching (RM) has been developed. This algorithm has allowed several ambiguities to be solved during the matching phases by imposing a smoothness constraint.

Finally, a Multi-Image Least Square Matching (MILSM) [16] has been performed for each extracted point. The MILSM has been implemented in order to improve the accuracy up to a sub-pixel dimension.

During the matching process, some blunders can be generated. These blunders are firstly deleted from the extracted edges using a filter that considers the relative point positions on the same edge: in particular, the position of a point is predicted considering the neighboring points of the edge and, then, the difference between the predicted and the real position of the point is evaluated. If the difference value is higher than a predefined threshold, the point is deleted. This filter is not robust: it will work well if the blunders are isolated from each other. For this reason, a second filter could be used to clean the edges when several blunders are present in a narrow space: this algorithm uses the point cloud information to verify the correctness of each dominant point: when it is out of a defined threshold from the point cloud, it is deleted.

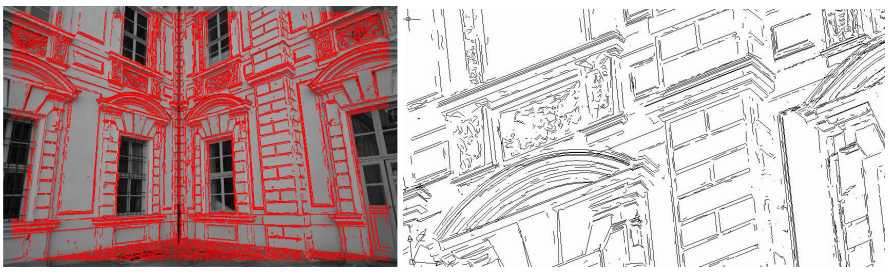

Fig. 5. Radiometric edges extracted before the point cloud validation (left) and geometrically validated and smoothed edges (Torino Valentino Castle test site)

Image matching allows radiometric edges to be extracted. Some of these edges are due to shadows or radiometric changes but they do not have a geometric correspondence. Only geometric boundaries are of interest in the survey for modeling purposes. For this reason, the position of each dominant point on the extracted edges is considered with respect to the point cloud: it is verified whether a geometric discontinuity occurs in the 3D model to the projected edge point.

The edges extracted by the matching algorithm are random noise affected and they cannot be directly used in the drawing production. For this reason, the noisy edges are split in basic elements (linear and curved elements), each element is smoothed and eased, in an automatic way, into lines, and second order curves by means of a polynomial fitting. Then, the basic elements are recollected in a unique smoothed edge [17].

Finally, geometric edges are exported in CAD environment in order to give preliminary data for the graphic drawing realization of the survey and for a rough evaluation of the achieved results.

3.3 First conclusions

Multi-image matching, if correctly integrated by the point cloud data, can give more affordable information than LiDAR technology for a modern Cultural Heritage 3D survey.

In the photogrammetric approach, the radiometric content is directly used to extract the geometric information while in the case of LiDAR techniques the color information is added as external information. In some way, the link between geometric and radiometric data is more effective in photogrammetry than in Point Cloud generation techniques such as LiDAR and ToF cameras.

The automation level offered by photogrammetry is higher than the one achievable by using traditional point cloud segmentation techniques. The manual intervention is reduced to few steps and the results are more complete and reliable than using only the point cloud information.

4 ToF camera point clouds and digital photogrammetry integration

Following the achieved results explained in the previous sections, and the same workflow, a practical test of break-line extraction by using the multi-image matching approach integrated with a ToF camera point cloud has been realized on a decorated window of the Valentino Castle test site (Torino, Italy).

Considering the technical characteristics of the SR-4000 camera, the test is limited to an architectural object that can be acquired with a limited number of ToF camera acquisitions.

The façades are painted and the texture is generally not good enough for the traditional image matching approach to be performed.

4.1 ToF data acquisition

After the camera warm-up, the SR-4000 camera was positioned on a photographic tripod and moved to different positions in order to achieve a complete coverage of the window to be surveyed (Fig.6).

According to the SR-4000 specifications, since the average distance between the camera and the window was about 3.5 m, the acquired area dimensions for each range image were about 3.00 m x 2.50 m.

In order to obtain a complete 3D model of the window (3 m large, 5 m high), the ToF data was acquired from six different positions, with an overlap of about 70% between the acquired range images.

Fig. 6. Three views of the surveyed window of the test site and SR-4000 data acquisition

4.2 ToF data processing

The distance of each pixel of the averaged frames was corrected with the distance error model proposed in [16], using a custom-made *Matlab*® application.

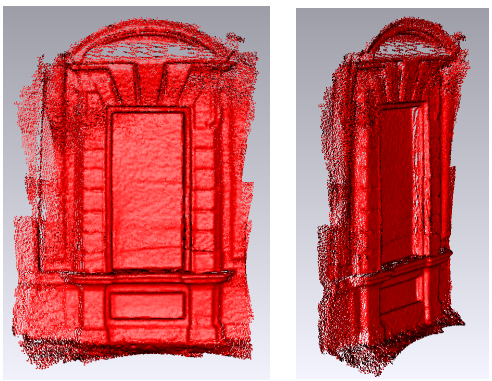

Fig. 7. Complete 3D ToF point cloud

The obtained point clouds were registered using the ICP algorithm implemented in

the *Geomagic Studio*® software in order to obtain a unique 3D model of the window.

In this way a dense Point Cloud (168551 points) was generated and then employed for the multi-image matching approach in order to extract the needed break-lines.

4.2 Image acquisition

The image acquisition was performed using the CANON EOS-5D MARK II digital camera equipped with a 24 mm lens. The taking distance was about 6 m. Five images were acquired according to an *ad hoc* configuration [17]. In Fig.8 an example of epipolar lines and correlation patches on the five images employed for the multi-image matching approach is reported.

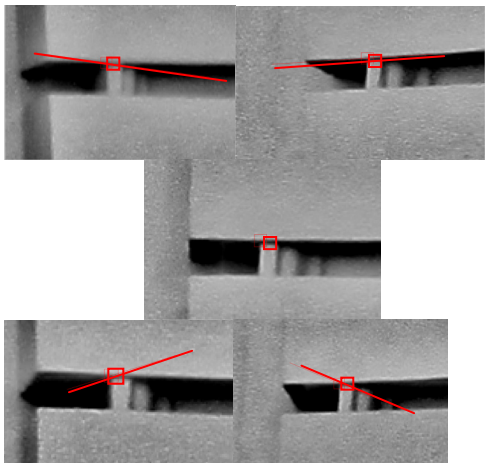

Fig. 8. Epipolar geometry of the acquired digital images

According to this particular configuration the epipolar lines run in tilted direction with respect to the main lines of the façade (horizontal and vertical), and the homologous points can be determined in an unambiguous way. Thanks to the image dimension (5616 x 3744 pixels) and the short taking distance, an excellent image resolution was reached (less than 2 mm of Ground Sample Distance (GSD)).

4.4 Data integration and results

The edge extraction allowed a complete set of lines to be defined from the reference image: Fig. 9 (left) shows the extracted edges, which are described by 45636 dominant points.

After the matching process, the position in the space of 32566 dominant points was defined. Only a percentage of 3% of these points was deleted after the blunder detection process. The resulting data was smoothed in order to ease the edges in lines and curves.

The result of this work is reported in Fig. 9 (right): it can be noticed that the

window geometry is complete and only some parts of the arcs are missing.

Fig. 9. Extracted and smoothed edges on the reference image

The smoothing correctly eased all the elements of the façade. In Fig.9 (right) a zoom of the final result is shown.

Obviously to produce useful representation drawings and/or 3D models a lot of works have to be done. Fig. 10 shows a 3D realistic model produced by using a LiDAR and Digital photogrammetry integration and the final drawing of a section.

5 Conclusions

The results of the researches carried out in the last few years by the Geomatics Research Group of the Politecnico di Torino for Cultural Heritage metric survey allow some final considerations to be outlined.

Fig. 17. From the results of a metric survey to the final drawing

Cultural Heritage metric survey essentially requires a geometric break-line definition. Point clouds of regular surfaces are generally not useful: the point clouds can give a proper answer to the metric survey requirements only when irregular and smoothed surfaces have to be described.

In the past the selection of points performed by a human operator using total stations, distance measurements and photogrammetric plotting forced the user to select the only necessary information during the acquisition and processing phases: the geometric points and break-lines which delimitate the surveyed objects were usually selected.

The new trend started with the LiDAR technique (and today with the ToF cameras), which changed the starting point of the process: the acquisition is made without any logic criteria, collecting millions of points and only the surveyor work allows useful information to be extracted. Unfortunately, as it is well known, the processing of point clouds in order to extract break-lines and affordable geometric descriptions (the true goal of a metric survey!) is not an easy task and a lot of work has to be still completed.

Multi-image matching is able to directly extract the geometry of the radiometric edges of a set of images but it usually finds a lot of troubles when high Z variations occur. The knowledge of an approximate 3D model of the surveyed object allows this problem to be overcome. Then, the point cloud (provided by LiDAR or ToF camera) is a good solution in order to distinguish between radiometric and geometric edges (the needed break-lines for a complete metric survey).

The ToF cameras represent a good alternative to LiDAR techniques to quickly produce point clouds with the same accuracy and precision.

Therefore, we can state that in the near future the 3D metric survey of Cultural Heritage will probably be performed by using multi-image matching and ToF point clouds: today technology allows this approach to be employed for object surveys where the taking distance is less than a tens of meters but in the near future the limitations in using these cameras will probably be solved.

Finally, considering the costs of digital and ToF cameras and their on-the-field easy management, the proposed approach will speed-up and simplify (from an economical point of view) the Cultural Heritage 3D metric survey.

References

1. Albota, M.A., Heinrichs, R.M., Kocher, D.G., Fouche, D.G., Player, B.E., Obrien, M.E., Aull, G.F., Zayhowski, J.J., Mooney, J., Willard, B.C., Carlson, R.R.: Three-dimensional imaging laser radar with a photon-counting avalanche photodiode array and microchip laser. Appl. Opt., 41, 7671--7678 (2002).
2. Baltsavias E.: Multiphoto Geometrically Constrained Matching. Phd. dissertation, ETH Zurich, Switzerland (1991)
3. Büttgen, B., Seitz, P.: Robust optical Time-of-Flight range imaging based on smart pixel structures. Trans. Circ. Sys, 1, 1512--1525 (2008)
4. Chiabrando, F., Chiabrando, R., Piatti, D., Rinaudo, F.: Sensors for 3D Imaging: Metric Evaluation and Calibration of a CCD/CMOS Time-of-Flight Camera. Sensors, n° 9, pp. 10080-10096 (2009)

5. Falie, D., Buzuloiu, V.. Noise characteristics of 3D Time-of-Flight cameras. In: Proceedings of IEEE Symposium on Signals Circuits & Systems (ISSCS), Iasi, Romania, pp. 229-232 (2007)
6. Habib, A. F., Ghanma, M. S., Tait, M.: Integration of LIDAR and photogrammetry for close range applications. In: International Archives of Photogrammetry and Remote Sensing, Vol. XXXIV/B2, Istanbul, Turkey (2004)
7. Kahlmann, T.; Remondino F.; Ingensand, H.: Calibration for increased accuracy of the range imaging camera Swiss Ranger. Int. Soc. Photogramm. Remote Sens. 2006, XXXVI, pp. 136-141 (2007)
8. Lange, R.: Time-of-Flight range imaging with a custom solid-state image sensor. In: Proceedings of SPIE Vol. 3823, pp. 180--191. Munich, Germany (1999).
9. Lange, R.: 3D Time-of-Flight distance measurement with custom solid state image sensors in CMOS/CCD-technology. Ph.D. Thesis, University of Siegen, Siegen, Germany (2000)
10. Lingua, A., Marenchino, D., Nex F.: Performance Analysis of the SIFT Operator for Automatic Feature Extraction and Matching in Photogrammetric Applications. Sensors, n° 9, pp. 3745-3766 (2009)
11. Lichti, D.: Self-Calibration of a 3D Range Camera. In The International Archives of the Photogrammetry, Remote Sensing and Spatial Information Sciences, Beijing, China, Vol. XXXVII, part B5, pp. 927-932 (2008)
12. Lindner, M.; Kolb, A.: Lateral and depth calibration of PMD-distance sensors. In: Proceedings of ISVC, Lake Tahoe, NV, USA, pp. 524-533 (2006)
13. Lingua A., Rinaudo F.: Aerial triangulation data acquisition using a low cost digital photogrammetric system. In: The International Archives of Photogrammetry and Remote Sensing, Vol. XXXIII/B2, pp. 449-454 (2000)
14. Nex, F.: Multi-Image Matching and LiDAR data new integration approach. PhD Thesis, Politecnico di Torino, Torino, Italy (2010)
15. Nex, F., Rinaudo, F.: New integration approach of Photogrammetric and LIDAR techniques for architectural surveys. In: Laserscanning 2009, Paris, France (2009)
16. Rochas, A., Gösch, M., Serov, A., Besse, P.A., Popovic, R.S.: First Fully Integrated 2-D Array of Single-Photon Detectors in Standard CMOS Technology. IEEE Photonic. Technol. Lett. 15, 963--965 (2003)
17. Weyer, C.A.; Bae, K.; Lim, K.; Lichti, D.: Extensive metric performance evaluation of a 3D range camera. Int. Soc. Photogramm. Remote Sens. XXXVII, pp. 939-944 (2008)
18. Zhang, L.: Automatic Digital Surface Model (DSM) generation from linear array images. Phd. dissertation, ETH Zurich, Switzerland (2005)